

# Anisotropy driven ultrafast nanocluster burrowing

P. Süle

Research Institute for Technical Physics and Material Science,  
Konkoly Thege u. 29-33, Budapest, Hungary,  
sule@mfa.kfki.hu, www.mfa.kfki.hu/~sule,

(Dated: February 5, 2008)

We explore the occurrence of low-energy and low-temperature transient cluster burrowing leading to intact cluster inclusions. In particular, the anomalously fast (ballistic) Pt nanocluster implantation into Al and Ti substrates has been found by molecular dynamics simulations using a tight-binding many-body potential with the 1 – 5 eV/atom low impact energy. Similar behavior has also been found for many other cluster/substrate couples such as Cu/Al and Ni/Ti, Co/Ti, etc. In particular, in Ni/Ti at already  $\sim 0.5$  eV/atom impact energy burrowing takes place. At this few eV/atom low impact energy regime instead of the expected stopping at the surface we find the propagation of the cluster through a thin Al slab as thick as  $\sim 50$  Å with a nearly constant speed ( $\propto 1$  eV/atom). Hence the cluster moves far beyond the range of the impact energy which suggests that the mechanism of cluster burrowing can not be explained simply by collisional cascade effects. In the couples with reversed succession (e.g. Ti/Pt, Al/Pt) no burrowing has been found, the clusters remain on the surface (the asymmetry of burrowing). We argue that cluster penetration occurs at few eV/atom impact energy when the cluster/substrate interaction is size-mismatched and mass anisotropic atomically.

PACS numbers: 36.40.Sx, 68.43.Jk, 68.35.Fx, 66.30.-h

## I. INTRODUCTION

Cluster deposition on solid surfaces has been the subject of intense atomistic level studies in the last decades<sup>1–7</sup>. The reason of the considerable interest is due to that recent progress in this field offers a great technological potential for the application of clusters in various areas, such as the smoothening and cleaning of surfaces<sup>8</sup>, the improvement of magnetic properties<sup>9</sup>, size-dependent catalytic activity<sup>10</sup>, thin film growth with a well-controlled grain size<sup>1–3</sup> or the formation of cluster assembled nanowires<sup>11</sup>.

Cluster-surface interaction as well as the mobility of clusters on surfaces have also been intensively studied<sup>3,12–15</sup>. Transient mobility (TM) of clusters has been known for a while on surfaces<sup>2,12,17,18</sup> but not in the bulk. Hereby we report on the possible occurrence of TM of various clusters perpendicular to the surface leading to transient cluster burrowing into various substrates. Until now only slow cluster burrowing with soft landing has been studied in few systems which takes place at least in a nanosecond time scale well above room temperature<sup>13–15</sup>. The high energy ion-bombardment induced burrowing of Pt nanoparticles into SiO<sub>2</sub> has also been reported recently<sup>16</sup>.

Cluster impact phenomena have been intensively studied by computer atomistic simulations to understand the processes which govern the creation of nanoscale structures on the surface<sup>1–4,6,7,13–15</sup>. However, at best of our knowledge no low-energy (few eV/atom or less) and low temperature cluster beam deposition with transient implantation rate has been reported until now in which the cluster remains intact in the bulk. Implantation of clusters with few tens of Å depth usually requires at least

few tens of eV impact energy<sup>2</sup> or even higher energy is required for deeper penetration depths<sup>6,7</sup>. Cluster implantation at much lower energies could offer great technological possibilities for the production of nanostructures due to the much less destructive conditions.

According to our recent findings that single atomic deposition in Pt/Al(111)<sup>19</sup> and interfacial intermixing in Pt/Ti bilayer<sup>20</sup> are anomalous in many respect, e.g. transient inter-layer atomic transport rates have been found, it could be that cluster transport in systems with the same atomic constituents could also be anomalously fast. Moreover, it has also been shown recently that in mass-anisotropic bilayers the enhancement of interfacial broadening and intermixing takes place<sup>22,23</sup> and it could also be that mass-anisotropy does influence the propagation of deposited clusters.

In this article we report on the occurrence of ultrafast cluster transport (burrowing) in Al (and in Ti, Ag and in Au) bulk upon low-energy impact ( $< \text{few eV/atom}$ ) at  $\sim 0$  K predicted by atomistic molecular dynamics (MD) simulations. The employed interpolated crosspotentials have been fitted to *ab initio* calculations. We show that the Pt cluster initialized with few eV/atom impact energy can move ballistically in the bulk of Al until few tens of ps. In other deposition events with various cluster/substrate couples we find similar behavior when the cluster to substrate interaction is atomically size mismatched and/or mass anisotropic in such a way that the cluster is composed of heavier and smaller atoms.

## II. THE SIMULATION METHOD

### A. General properties

Classical constant volume tight-binding molecular dynamics simulations<sup>26</sup> were used to simulate soft landing and low-energy cluster impact of various nanoclusters on (111) surfaces of Al, Ti, Ag and Au at  $\sim 0$  K initial temperature using the PARCAS code<sup>4,13,27</sup>. The MD code has widely been used for the study of various atomic transport phenomena in the last few years<sup>4,13,19,20,22,27</sup>. Although we carry out simulations at  $\sim 0$  K, we find a substantial local heating up in a local surface region of Al, hence the correct dissipation of the emerged heat should be handled using temperature control. A variable timestep and the Berendsen temperature control is used at the cell border<sup>28</sup>. The simulation uses the Gear's predictor-corrector algorithm to calculate atomic trajectories<sup>27</sup>. The maximum time step of 0.05 fs is used during the operation of the multiple time step algorithm. The system couples to a heat bath via the damping constant to maintain constant temperature conditions and the thermal equilibrium of the entire system<sup>28</sup>. The time constant for temperature control is chosen to be  $\tau = 70$  fs, where  $\tau$  is a characteristic relaxation time to be adjusted<sup>28</sup>. The Berendsen temperature control has successfully been used for nonequilibrium systems, such as occur during ion-bombardment of various materials<sup>4,13,20,22,27</sup>.

For simulating deposition it is appropriate to use temperature control at the cell borders. This is because it is physically correct that potential energy becomes kinetic energy on impact, i.e. heats the lattice. This heating should be allowed to dissipate naturally, which means temperature control should not be used at the impact point. Periodic boundary conditions are imposed laterally. The observed anomalous transport processes are also observed without periodic boundary conditions and Berendsen temperature control. Further details are given in<sup>27</sup> and details specific to the current and similar systems in recent communications<sup>19,20,22</sup>.

The top of the simulation cell is left free (the free surface) for the deposition of Pt atoms. The bottom layers are held fixed in order to avoid the rotation of the cell. Since the z direction is open, rotation could start around the z axis. The bottom layer fixation is also required to prevent the translation of the cell. In few cases, however, we do not fix bottom layers, when the penetration of the deposited cluster through thin substrate films has been demonstrated. No rotation of the cell has been found in these cases.

The size of the typical simulation cell for the Pt/Al system is  $80 \times 80 \times 42 \text{ \AA}^3$  including 16128 substrate atoms (with a fcc lattice, 15 active MLs are supported on 3 fixed bottom monolayers (MLs)). We also tried substrates with different lateral sizes ( $80 - 160 \text{ \AA}^3$ ) and slab thickness ( $42 - 100 \text{ \AA}^3$ ) up to  $\sim 150000$  number of atoms.

TABLE I: The parameters used in the interpolated tight binding potential (TB-SMA) given in Eqs. (1)-(2)<sup>26</sup>. The parameters of the crosspotential have been obtained as follows using an interpolation scheme<sup>22</sup>: For the preexponentials  $\xi$  and  $A$  we used the harmonic mean  $A_{AlPt} = (A_{Al} \times A_{Pt})^{1/2}$  for  $q$  and  $p$  we use the geometrical averages:  $q_{AlPt} = (q_{Al} + q_{Pt})/2$ . The first neighbor distance of the Al-Pt potential is given also as a geometrical mean of  $r_0 = (r_0^{Pt} + r_0^{Al})/2$ . In order to get better agreement between *ab initio* and semiempirical potentials parameters  $\xi$  and  $r_0$  have been optimized. In the case of Co/Au parameter  $q$  has also been fitted.

	$\xi$	q	A	p	$r_0$
Al-Pt	2.7	3.258	0.191	9.612	3.0
Ti-Pt	4.2	2.822	0.149	11.015	2.87
Ni-Ti	0.8	1.416	0.052	14.209	2.72
Cu-Al	2.1	2.397	0.102	9.785	2.85
Co-Au	2.5	2.7	0.140	10.917	2.85

Other cluster/substrates couples (Pt/Ti, Co/Au, Cu/Al, Ni/Ti) together with reversed succession (Ti/Pt, Ti/Ni, etc.) have also been constructed with similar system size. We tested cluster impact on much larger substrates and find no dependence of the anomalous atomic transport properties of the deposited atoms on the finite size of the simulation cell. The cubic cluster includes roughly  $\sim 1500$  atoms (the length of cube edges:  $\sim 30 \text{ \AA}$ ). We also tested the penetration of various clusters in different substrates with similar lateral size and slab thickness and cluster size. The kinetic energy of the deposited particles is in the range of  $\sim 1 - 10$  eV/atom (the velocity of the clusters normal to the surface is  $v \approx 20 - 200 \text{ \AA/ps}$ ). The cluster is initialized at  $\sim 8 \text{ \AA}$  above the (111) surface of the substrate.

### B. The interatomic potentials

We use the many-body Cleri-Rosato (CR) parametrization of the tight-binding second-moment approximation (TB-SMA) interaction potential to describe interatomic interactions<sup>26</sup>.

Within the TB-SMA, the band energy (the attractive part of the potential) reads,

$$E_b^i = - \left[ \sum_{j, r_{ij} < r_c} \xi^2 \exp \left[ -2q \left( \frac{r_{ij}}{r_0} - 1 \right) \right] \right]^{1/2}, \quad (1)$$

where  $r_c$  is the cutoff radius of the interaction and  $r_0$  is the first neighbor distance (atomic size parameter).

The repulsive term is a Born-Mayer type phenomenological core-repulsion term:

$$E_r^i = A \sum_{j, r_{ij} < r_c} \exp \left[ -p \left( \frac{r_{ij}}{r_0} - 1 \right) \right]. \quad (2)$$

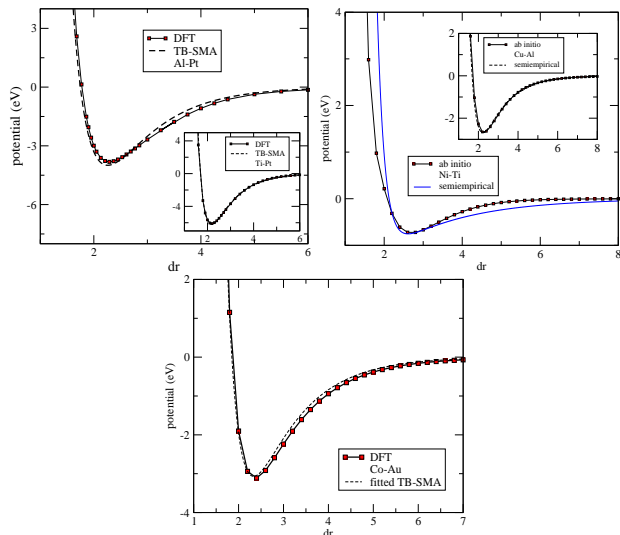


FIG. 1: The crosspotential energy (eV) for the dimers Al-Pt, Ti-Pt (inset Fig. 1a), Ni-Ti, Cu-Al (inset Fig. 2a) and Co/Au as a function of the interatomic distance (Å) obtained by the *ab initio* PBE/DFT method. For comparison the fitted interpolated semiempirical potentials (TB-SMA) are also shown. The fit procedure has been carried out by varying parameters  $\xi$  and  $r_0$  in order to get the best match of the potential energy curves with the *ab initio* one.

The parameters ( $\xi, q, A, p, r_0$ ) are fitted to experimental values of the cohesive energy, the lattice parameter, the bulk modulus and the elastic constants  $c_{11}$ ,  $c_{12}$  and  $c_{44}$ <sup>26</sup> and which are given in Table 1. The summation over  $j$  is extended up to fifth neighbors for fcc structures<sup>26</sup>. The cutoff radius  $r_c$  is taken as the third neighbor distance for all the interactions. We tested the Al-Al and the Al-Pt potential at cutoff radius with larger neighbor distances and found no considerable change in the results. This type of a potential gives a very good description of lattice vacancies, including migration properties and a reasonable description of solid surfaces and melting<sup>26</sup>. We also tested the Al-Al and the Al-Pt potential at cutoff radius with larger neighbor distances and found no considerable change in the results<sup>23</sup>. The cutoff radius is taken as the third-fourth neighbor distance ( $r_c \approx 10 - 15$  Å) for all the interactions which we find sufficiently large enough.

For the crosspotential of substrate atoms and Pt we employ an interpolation scheme<sup>22</sup> using the geometrical mean of the elemental energy constants and the harmonic mean for the screening length are taken as in refs.<sup>22</sup>. The CR elemental potentials and the interpolation scheme for heteronuclear interactions have widely been used for MD simulations<sup>14,21,22</sup>. Recently a CR interpolated crosspotential has also successfully been used for Ti/Pt in agreement with our experimental results<sup>20</sup>. The scaling factor  $r_0$  (the heteronuclear first neighbor distance) is calculated as the average of the elemental first neighbor distances. The AlPt potential has been fitted to the measured effective heat of mixing in the cubic

AlPt ( $\Delta H \approx -100$  kJ/mol)<sup>22</sup>. The melting temperature of 1870 K<sup>30</sup> is reproduced by our Cleri-Rosato crosspotential within the range of  $1800 \pm 100$  K. In order to adjust  $\Delta H$  in the Al-Pt potential (which is proportional to the strength of the interaction and to the heat of alloying in the AlPt alloy) the preexponential parameter  $\xi$  in Eq (3) is set to  $\xi \approx 3.0$ <sup>23</sup>. Further details are given in<sup>27</sup> and details specific to the current system in recent communications<sup>20,22,23</sup>.

In order to check the accuracy of the employed interpolated crosspotentials, the crosspotential energy has also been calculated for few of heteronuclear pairs (Al-Pt, Ti-Pt, Ni-Ti, Cu-Al, Co-Au) using *ab initio* local spin density functional calculations<sup>31</sup> together with a quadratic convergence self-consistent field method. The G03 code is well suited for molecular calculations, hence it can be used for checking pair-potentials. The interatomic potential  $V(dr)$  between two atoms is defined as the difference of total energy at an interatomic separation  $dr$  and the total energy of the isolated atoms

$$V(dr) = E(dr) - E(\infty). \quad (3)$$

The Kohn-Sham equations (based on DFT)<sup>32</sup> are solved in an atom centered Gaussian basis set and the core electrons are described by effective core potentials (using the LANL2DZ basis set)<sup>33</sup> and we used the Perdew-Burke-Ernzerhof (PBE) gradient corrected exchange-correlation potential<sup>34</sup>. First principles calculations based on density functional theory (DFT) have been applied in various fields in the last few years<sup>35</sup>. The obtained profiles are plotted in Fig. 1 together with our interpolated semiempirical many-body TB-SMA potentials for the various dimers. Our interpolated potential is partly fitted to the *ab initio* one: parameters  $\xi$  and  $r_0$  have been varied to get the best matching. We find that our fitted interpolated TB-SMA potentials match reasonably well the *ab initio* one hence we are convinced that the TB-SMA model accurately describes the heteronuclear interaction in the Al-Pt dimer. Even if we use the interpolated TB-SMA without fitting, we get nearly the same results which indicates that the interpolation scheme is effective. We assume that the fitted diatomic potential is transferable for those cases when a cluster atom is embedded in the substrate. Heteronuclear interactions can be reasonably well described by dimer potentials during interfacial interactions while pair potentials are less accurate in alloy phases where the local number of crossinteractions is much larger than 1.

In Figs 1a-1c we show the *ab initio* DFT potential energy curves and the fitted interpolated ones. In most of the cases we could reach a fairly good agreement which might increase the credibility of the employed approach. We also carried out simulations for couple of other cluster/substrate pairs and for which we use the simple interpolation scheme for the crosspotential. Results for these pairs are shown in the discussion section.

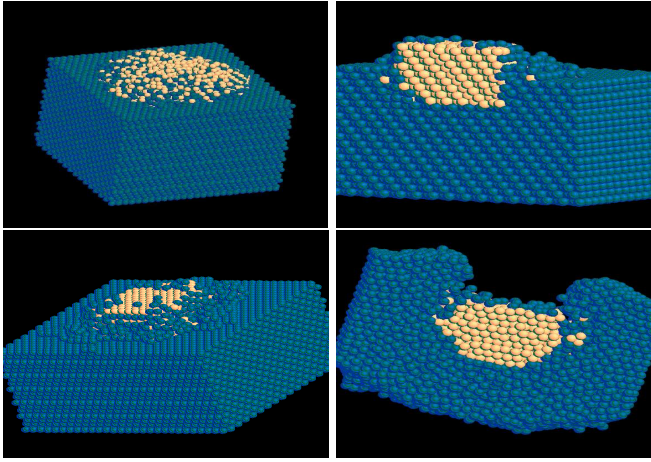


FIG. 2: The cartoons of the simulation cells obtained after the impact of Co cluster on Au(111) and Pt nanocluster on Al(111). The atoms with lighter color are the cluster atoms. From right to left: *fig. 2a*: the top view of the simulation cell of Co cluster on Au(111) impact event after 5 eV/atom impact. *fig. 2b*: the burrowed (embedded) Pt cluster in Al (crosssectional view, 1eV/atom impact), *fig. 2c*: the top view of the burrowed Pt cluster, *fig. 2d*: the crosssectional slab (cut in the middle of the cell) of the Al(111) substrate after the penetration of the implanted Pt cluster (5 eV/atom impact energy). Figs. 2a-2c have been plotted after few tens of ps the cluster impact. In Fig. 2d the snapshot is plotted at 5 ps.

### III. RESULTS

The low-energy deposition (1 – 5 eV/atom) of nanoclusters of Pt on Al(111) and Ti leads to the unexpected ultrafast cluster sinking and burrowing within few ps<sup>29</sup>. The process can be considered as an athermal transient transport which takes place in nearly 0 K simulations within a ps at few eV/atom impact energy. We find a similar behavior for other cluster/substrate couples such as Cu/Al, Ni/Al, Ni/Ti or Co/Ti, etc. Common feature of these couples is the large atomic size or mass anisotropy (the host atoms are large and light and the cluster atoms are smaller and heavy).

Normally, most of the clusters should stop and fall apart and spread on the surface or in the upper layers at this energy regime (see e.g. in the review article<sup>2</sup> or in refs.<sup>3,6,7</sup>). Actually, this feature of cluster impact can be used for thin film growth<sup>1-3</sup>. In this article, this has been demonstrated for the Co cluster deposition on Au(111) in Fig. 2a and can also be seen at a web page<sup>29</sup>. In this case we find the fragmentation of the Co cluster upon impact on Au(111) at 5 eV/atom impact energy. We expect for most of the low-energy cluster deposition events with various substrates and clusters the stopping of the cluster on the surface (with only weak penetration). Even for higher impact energies we find no penetration of Co to Au (up to few tens of eV/atom). At 5 eV/atom energy the Co nanoparticle falls apart and an intermixed

nanodot remains on the surface.

Also, no burrowing occurs for the couples with reversed succession: e.g. the energetic deposition of Ti cluster on Pt substrate leads to trapping on the surface with some fragmentation and/or spreading on the surface (similar situation takes place for Al/Pt and Ti/Ni, etc.)<sup>29</sup>. Hence the ultrafast burrowing of clusters is asymmetric with respect to the interchange of the atomic constituents.

Clearly we find a different and anomalous situation for Pt cluster on Al(111) and for the other couples under study (Pt/Ti, Ni/Ti, Cu/Al). Instead of the normal cluster low-energy impact behavior the Pt cluster keeps its integrity during the impact and starts to burrow (penetrate) ballistically below the surface instead of stopping at the surface. Below 1 eV/atom the stopping or the partial penetration of the Pt clusters has been found which implies that the burrowing has a potential energy barrier of  $\sim 1$  eV/atom.

Penetration of clusters upon impact has only been found until now at much higher impact energy above  $\sim 15$  eV/atom which takes place together with the fragmentation of the cluster<sup>2,6,7</sup>. Hence no burrowing process takes place and the higher implantation energy of the clusters lead to the serious damage of the cluster and the substrate. E.g. the amorphization of size-selected Au, Ag, and Si clusters have been found in graphite at few keV implantation energy<sup>6,7</sup>. Our finding is also different from the cases found for Co cluster burrowing in Cu. In this case the cluster penetration (CP) is relatively slow process and takes place in a ns time scale and is a thermally activated process<sup>13</sup>.

It should also be stressed that the Pt cluster remains also intact at higher impact energies. In Figs. 2b-2c the cartoons of the burrowing event is shown for the case when the cluster is initialized by 1 eV/atom kinetic energy. The sinking of the cluster takes place in few ps (ballistic process). Increasing the impact energy up to 5 eV/atom the sinking process continues and the cluster penetrates through a  $\sim 50$  Å thick Al or Ti slab (Fig. 2d) in 10 ps. The cluster travels through the thin substrate slab with a nearly constant speed ( $\sim 1$  eV/atom) and remains nearly intact when leaves the bottom of the thin slab. The corresponding animations can be seen in a web page<sup>29</sup>. In Fig. 2d we show a snapshot of cluster implantation at 5 ps.

Hence the stopping of the Pt cluster does not occur as it should be in most of other cluster impact events (such in the case of Co cluster on Au or for Al cluster on Al). In the case of Co cluster on Au(111) we see the complete disintegration of the Co cluster on the surface (Fig. 2a) even at 5 eV/atom impact energy. At 5 eV/atom impact energy the Pt cluster penetrates far beyond the range of the deposited energy (that is few Å) into the substrate by an order of magnitude larger implantation depth. Therefore, simple collisional cascade effects can not explain the enhancement of the vertical cluster mobility. Therefore, there must be a specific mechanism which weakens stopping effects for the Pt/Al, Pt/Ti for other couples.

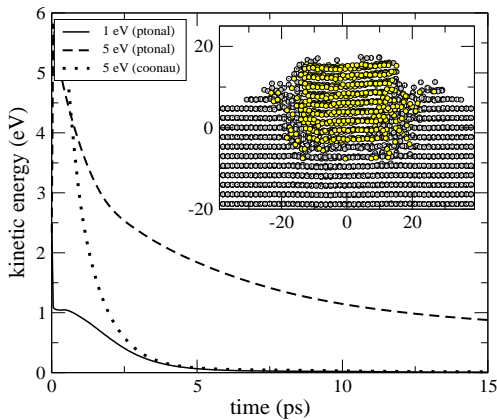


FIG. 3: The average kinetic energy (eV/atom) of the penetrating Pt cluster as a function of the simulation time (ps) during complete penetration through the Al slab (the slab thickness is  $\sim 50$  Å). *Inset*: The crosssectional view of the crosssectional slab of the burrowed Pt cluster in Al at 1 eV/atom impact energy cut in the middle of the simulation cell.

In Fig. 3 the average (downward) kinetic energy of the moving (burrowing) cluster per atom is also shown for a typical transient cluster burrowing (TCB) event at 5 eV/atom initial kinetic energy. The cluster slows down to  $\sim 1$  eV/atom after the impact and continues moving through the Al slab. Contrary to this, the Co cluster stops immediately after the impact and the kinetic energy of the cluster drops sharply to zero at the same initial impact energy. In the case of 1 eV/atom impact energy we find burrowing for Pt on Al and no further penetration is seen which indicates that complete cluster penetration has a barrier of few eV/atom. The crosssectional view of the embedded cluster is shown in the inset Fig. 3 at the end of the simulation which shows us that the cluster remains largely intact during burrowing. Also, even no partial cluster burrowing occurs below  $\sim 0.5$  eV/atom impact energy.

In Fig. 4 we show the calculated penetration depth  $d_p$  of clusters obtained during various impact events making statistics as a function of the impact energy up to 10 eV/atom. We find the nearly linear increase of  $d_p$  with  $E_{imp}$ . This is in accordance with the finding of Praton *et al.*<sup>6,7</sup> as they found the nearly linear scaling of the implantation depth of Au, Ag, and Si clusters into graphite as a function of the impact energy in the keV impact energy regime. We find this scaling relation at much lower impact energy (few eV/atom regime). In the Inset Fig. 4 the linear scaling of the kinetic energy of penetration ( $E_{pen}$ , propagation) can be seen as a function  $E_{imp}$ . These features show us that both  $d_p$  and  $E_{pen}$  scales linearly with  $E_{imp}$ .

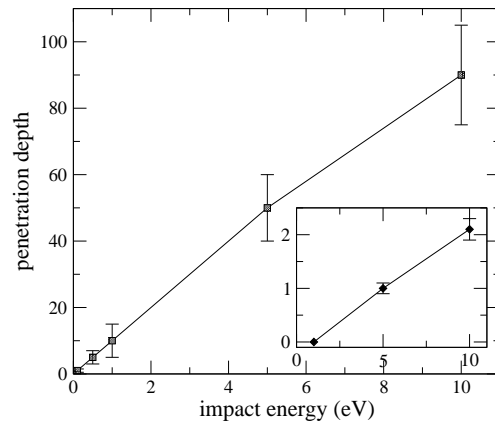


FIG. 4: The penetration depth ( $d$  in Å) of various cluster impact events as a function of the impact kinetic energy. Error bars denote standard deviations obtained during various events (statistics). *Inset*: The average kinetic energy of penetration of cluster atoms (eV/atom) through the substrate as a function of the impact kinetic energy (eV/atom).

#### IV. DISCUSSION

Interestingly, the observed anomalous processes (transient burrowing, the asymmetry of CP) are only weakly sensitive to the choice of the heteronuclear potential. We get similar results for the interpolated and for the fitted potentials. At first sight this is surprising, however, we find that not the strength of the crossinteraction built in the crosspotential determines cluster mobility. This is in accordance with recent findings in similar systems for atomic deposition events<sup>19</sup> and for ion-beam intermixing<sup>22</sup>. The variation of parameter  $\xi$  in Eq. (1) does not affect significantly the final results in accordance with earlier findings during ion-mixing of the Ti/Pt bilayer<sup>22</sup>. Parameter  $\xi$  is proportional to the built in heat of mixing of the corresponding alloy phase<sup>22</sup>. Atomistically, it determines the deepness of the potential energy well, hence the strength of the heteronuclear interaction. The possible reason of this insensitivity to the strength of the crossinteraction is that transient (ballistic) and athermal atomic transports are only weakly sensitive to pair-interactions e.g. between colliding ballistic particles e.g. in a collisional cascade. In other words, not chemical interdiffusion (chemical forces) and thermochemistry (heat of mixing) determine the magnitude of bulk cluster mobility (and the implantation or penetration depth). CP occurs e.g. in Pt/Al either for weakly repulsive and for attractive crosspotentials.

##### A. Mass-effect and cluster penetration

It turned out during comparing the penetration depths obtained for various cluster/substrate pairs that atomic mass anisotropy, that is the atomic cluster to substrate



mass ratio ( $\delta$ ) could seriously influence CP and could be responsible for the apparent asymmetry in CP with respect to the interchange of the cluster and substrate constituents.

Since we find that atomic mass ratio could be an important ingredient of CP we briefly summarize our recent results in which we find the strong effect of mass anisotropy on interdiffusive behaviors of various film/substrate systems<sup>22</sup>. The enhancement of atomic penetration (intermixing) has also been reported recently of Pt in Ti substrate during ion-sputtering of Pt/Ti film/substrate system<sup>20</sup>. The asymmetry of interdiffusion in Pt/Ti with respect to the succession of the film and substrate has also been found<sup>20</sup>. In few other recent publication we also explained the enhanced atomic transport with mass-effect<sup>22,37</sup>.

It might be the case that similar mass ratio driven thermalization appears during CP. Indeed, if we set in artificial mass isotropy in burrowing systems, we get a much weaker cluster penetration. Moreover, if we interchange artificially atomic masses between Al and Pt, we get no CP. Hence we find that the inversion of mass-anisotropy in the system hampers the enhancement of cluster mobility and CP. Moreover, if we interchange atomic masses in the Co/Au system, we does get, CP. In mass isotropic systems, in which no cluster penetration occurs, such as Ni/Cu or Co/Cu, ultrafast CP can also be induced by setting in artificial mass anisotropy. These simulation results strongly suggest that mass anisotropy could be a decisive parameter in cluster implantation.

The role of mass effect in CP might be due to collisional cascade effects. When cluster impact occurs the initialization of local melting could not appear with atomic mass ratio  $\delta = \frac{m_{cl}}{m_{subs}} \leq 1$ , where  $m_{cl}$  and  $m_{subs}$  are the atomic masses in the cluster and in the substrate. This is simply due to backscattering effects when  $\delta \leq 1$ : light atoms stop at an interface composed of heavy atoms at low impact energies in a similar way as it has been found for intermixing during the ion-bombardment of various bilayers<sup>22</sup>. In the case of  $\delta \approx 1$ , however, the dissipation of the impact energy into the lattice is the most effective<sup>22</sup>, and no thermalization or only a short lived collisional cascade takes place which does not allow CP. However, when  $\delta \geq 1$ , local thermalization of the substrate will appear because heavier cluster atoms penetrate into the substrate top layer.

The effect of  $\delta$  on CP can be demonstrated more quantitatively if we vary  $\delta$  artificially e.g. in a nearly mass and atomic size isotropic system, such as Co/Cu and plot the penetration depth as a function of  $\delta$ . We use for simulations a standard Cleri-Rosato set of parameters<sup>26</sup> and a fitted potential for the Cu-Co interaction<sup>36</sup>. In principle we can get a universal plot, which holds more or less precisely for any kind of cluster/substrate couples in which mass anisotropy governs CP. In Fig. 5 we show with closed symbols those values which are obtained for those couples, which composed of atoms with moderate lattice mismatch (e.g. in Cu/Ti, Pt/Al, Au/Al, Pt/Ag, Ti/Al

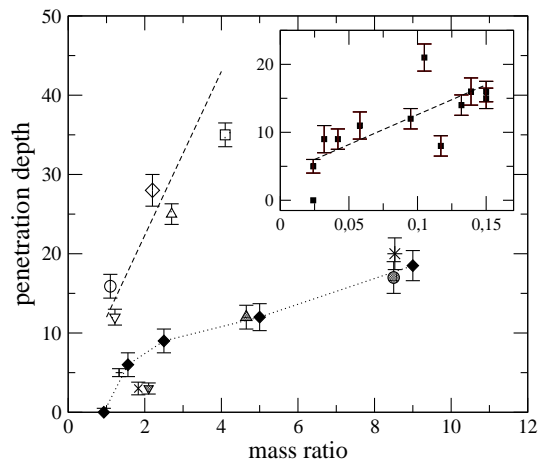


FIG. 5: The penetration depth ( $d_{pen}$  in Å) of various cluster impact events (2 eV/atom) as a function of mass ratio ( $\delta$ ,  $\delta \geq 1$ ). Error bars denote standard deviations obtained during various events (statistics). Filled diamonds correspond to values obtained for the Co/Cu couple. The dotted line is for guiding eyes. Plus, circle, star, cross, triangle down and triangle up denote Cu/Ti, Pt/Al, Au/Al, Pt/Ag, Ti/Al and Au/Ag, respectively. Opened symbols: Results are shown with opened circle, diamond, triangle down, triangle up and square for Ni/Ti, Ni/Al, Co/Ti, Cu/Al and for Pt/Ti, respectively. A linear fit has also been plotted with a dashed line to guide eyes. Inset: The penetration depth (Å) as a function of the lattice mismatch  $\epsilon$  ( $\epsilon > 0$ ) for various cluster/substrate couples which are the followings:  $\epsilon = 0.024$ , Cu/Co, 0.058, Pt/Ti (iso), 0.04, Pt/Ag (iso), 0.10, Ni/Pd (iso), 0.11, Cu/Al (iso), 0.12, Cu/Ag (iso), 0.132, Cu/Ti, 0.14, Ni/Ag (iso), 0.15, Co/Ti, 0.15, Ni/Ti, 0.15, Co/Ti, 0.15, Ni/Ti, where (iso) denotes artificial mass isotropic calculations.

and Au/Ag). These systems give  $d_{pen}$  values around the curve obtained for Co/Cu.

## B. The role of lattice mismatch

However, in those cases, in which both cluster to substrate lattice mismatch ( $\epsilon = (a_s - a_{cl})/a_s > 0$ , where  $a_s$  and  $a_{cl}$  are lattice constants of the substrate and cluster constituents) and mass anisotropy are considerable (Co/Ti, Ni/Al, Pt/Ti, Cu/Al) a deviation from the curve of Co/Cu can be seen (opened symbols and dashed fitted curve). Hence we are faced with the splitting of the  $d_{pen}$  vs.  $\delta$  plot into two regimes. These regimes can be understood as the separation of  $\delta$  and  $\epsilon$  dependent TCB processes. This is simply due to the fact that one hardly can find systems in which both  $\delta$  and  $\epsilon$  is robust. In strongly mass-anisotropic couples with  $\delta \gg 1$  usually  $\epsilon$  is not that pronounced. When lattice mismatch is robust in such a way that the cluster atom is the smaller ( $\epsilon < 0$ ) mass anisotropy is not that robust as possible in other cases. Hence the frequency of the appearance of strongly mass anisotropic and lattice mismatched ( $\delta, \epsilon$ )

couples among various possible cluster/substrate pairs is constrained by nature.

In the nearly mass-isotropic Ni/Ti and Co/Ti only a smaller deviation can be seen, in Fig. 5 although still a considerable penetration occurs in these size-mismatched couples. In particular, the Co nanocluster burrows into the Ti phase temporarily completely and is ejected closer to the surface finally with  $d_{penet} \approx 16 \pm 1.5$  Å. However, no penetration takes place for the reversed cases (Ti/Ni, Ti/Co).

*We argue than in this paper that atomic size mismatch (ASM, also we call it atomic size anisotropy) could be together with  $\delta$  the basic parameters which govern cluster mobility and TCB in the bulk.*

### C. Burrowing clusters: atomic size mismatch and cluster bulk mobility

Using MD simulations it has been shown recently that the ratio of the cluster lattice parameter to the substrate lattice constant (that is  $\epsilon$ ) has significant effect on cluster diffusion on the surface (interfacial incommensurability)<sup>2,25</sup>. In the rest of the paper we argue that transient cluster burrowing and bulk mobility could also depend on  $\epsilon$ . The possible operation of a  $\epsilon$ -dependent mechanism is supported by various simulations with mass isotropic and lattice mismatched systems (e.g. Co/Ti, Ni/Ti, etc.) which also show up transient cluster burrowing.

Varying the elements in the cluster and substrate we can reach the conclusion that ASM could also be a key parameter in TCB. In particular, in the Ni/Cu system we get no TCB ( $\epsilon \approx 0.02$ ), while if we replace Cu with Ti, TCB does occur in Ni/Ti ( $\epsilon \approx 0.15$ ). The former couple is a nearly mass and size isotropic system, while the latter one is size anisotropic being a considerable atomic volume difference between Ni and Ti. Also, no TCB occurs in the Ti/Ni system, when Ni is the substrate and Ti is the cluster. The larger Ti atoms can not penetrate to the Ni phase. These situations support the ASM driven mechanism when  $\delta \approx 1$ . Also, an artificially set mass isotropy e.g. in Pt/Al ( $\epsilon \approx 0.06$ ) does not suppress completely CP, hence there must be another system parameter which drives CP even in mass-anisotropic couples. Co/Ti provides another mass isotropic and size anisotropic example in which TCB occurs. Finally, if we deposit Ti cluster on Al, no TCB occurs in accordance with the expectations (size isotropic couple).

These results are summarized in the Inset Fig. 5 in which the penetration depths of various cluster/substrate couples at 2 eV/atom impact energy have been plotted against the cluster to substrate lattice mismatch  $\epsilon$ . In the mass anisotropic cases in order to exclude mass effect on CP and to study purely the effect of lattice mismatch on CP an artificial mass isotropy has been imposed (iso). We assume that lattice mismatch and mass anisotropy have a nearly independent effect on CP, and their con-

tributions to the total penetration depth  $d_{pen}$  can be summed up from individual terms:  $d_{pen} = d_{pen}^{\delta} + d_{pen}^{\epsilon}$ , where  $d_{pen}^{\delta}$  and  $d_{pen}^{\epsilon}$  are the mass anisotropy and atomic size mismatch induced contributions to transient cluster penetration. Hence during mass isotropic simulations  $d_{pen} \approx d_{pen}^{\epsilon}$ . We find a nearly linear dependence for various couples which supports the assumption that CP might depend on  $\epsilon$ .

In few of the cases, however, deviation from the linear dependence has also been found (Cu/Ag, Cu/Al). We find the strongest transient burrowing process in iso-Cu/Al while in iso-Cu/Ag the penetration depth drops below the fitted curve. In these cases it could be that not only anisotropy parameters govern CP, it could be that hidden (unknown) parameter(s) also contribute to CP. For vanishing lattice mismatch ( $\epsilon < 0.03$ )  $d_p$  vanishes abruptly if  $\delta = 1$  (mass isotropy).

### D. Nonburrowing clusters

We summarize hereby the general properties of nonburrowing cluster/substrate pairs. In general, in these couples cluster penetration and implantation can only be induced at least with few tens of eV/atom impact energy. For instance, in the Co/Cu system we find complete implantation at  $\sim 50$  eV/atom energy, however, the cluster loses its integrity and even the substrate experiences serious damage. Hence, the technological applicability of this energy regime is questionable.

As it has already been shown for many examples, the interchange of atoms in a burrowing cluster/substrate couple might lead to a nonburrowing couple. In these couples  $\epsilon < 0.0$  (negative lattice mismatch) and/or  $\delta \leq 1$  (mass isotropy,  $\delta \approx 1$  or inversed mass anisotropy,  $\delta < 1$ ). The nonburrowing  $\epsilon < 0.0$  couples are those A/B systems in which A=Al, Ti, Ag, Au and B=Cu, Ni, Co, Pt. Hence  $\epsilon < 0.0$  together with  $\delta < 1$  have a strong suppressive effect on TCB independently from each other. The deposited cluster remains on the surface and  $d_{pen} \approx 0$  when  $\delta < 1$  and/or  $\epsilon < 0.0$ . In these cases penetration does not occur even temporarily. In many other mass-isotropic ( $\delta \approx 1$ ) and size-anisotropic cases ( $\epsilon > 0.0$ ) clusters first burrow deeply into the substrate (e.g. in Co/Ti) and then are ejected to the surface or to the top layers.

The thermally induced burrowing of Co clusters into Au(111) surface has been studied recently<sup>24</sup>. The experimentalists claim that Co clusters possess a strong tendency to bury themselves into Au substrate<sup>24</sup>. Since this process can only be activated above room temperature annealing, we repeated our simulation for Co/Au with simulating the annealing process and indeed the partial burrowing of the Co cluster has been found at 450 K, although the cluster does not keep its integrity completely and sinks only few monolayer deep into the substrate. We conclude that in Co/Au the experimentally observed burrowing might not be an athermal process

(TCB) and could be similar to that of reported in the Co/Cu couple<sup>13</sup>. In the size-mismatched Co/Au system although  $\epsilon = 0.13$ , however,  $\delta \ll 1$ , hence Co clusters are stopped at the Co/Au interface. The stopping power of  $\delta \ll 1$  is a stronger effect than the burrowing effect of lattice mismatch. Hence we conclude from this that the effect of ASM can only be realized when  $\delta \geq 1$ . This has been demonstrated with an artificially inverted  $\delta$  (the atomic masses of the cluster and substrate atoms have been interchanged) with which we can induce ultrafast CP in Co/Au. It is also clear that no penetration appears in Au/Co, although  $\delta > 1$ . In this case this is due to the stopping power of  $\epsilon < 0$ . Hence  $\delta \ll 1$  and  $\epsilon < 0$  suppress TCB.

## V. CONCLUSION

In conclusion, we explore the occurrence of transient nanocluster penetration (burrowing) in various substrates using atomistic simulations at low energy cluster impacts. We point out that the cluster to substrate atomic mass and size anisotropy plays a significant role in the mass transport: clusters with heavier and smaller atoms burrow into a substrate composed of lighter and larger atoms. The transient burrowing process is largely insensitive to the strength of cross-interaction (that is

proportional to the heat of mixing) and is driven by the atomic mass ratio and lattice mismatch.

The deep penetration of metallic clusters into metallic substrates could allow the preparation of metallic inclusions and buried nanostructures implanted into the substrate. Beyond the possible technological application of cluster burrowing, the explored new phenomenon could also be interesting in a theoretical point of view. In particular, the understanding of transient cluster mobility in the bulk could contribute to the advance of the emerging new field of anomalous diffusion (see refs.<sup>19,20</sup> and references therein). These peculiar results provide new evidences to the new concept that atomic transport could become anomalous in the nanoscale under not yet clearly established conditions<sup>38</sup>. Common feature of few of these processes the athermal characteristics (non-Arrhenius atomic transport) and that the deposit-surface interaction is largely independent of chemical forces<sup>19,22</sup>.

## VI. ACKNOWLEDGMENT

This work is supported by the OTKA grants F037710 and K-68312 from the Hungarian Academy of Sciences. We wish to thank to K. Nordlund, T. Michely and to M. Menyhárd for helpful discussions. The help of the NKFP project of 3A/071/2004 is also acknowledged.

- 
- <sup>1</sup> Karl-Heinz Meiwes-Broer (Ed.), *Metal Clusters at Surfaces: Structure, Quantum Properties, Physical Chemistry* (Springer Series in Cluster Physics, Berlin, 2000).
  - <sup>2</sup> P. Jensen, Rev. Mod. Phys. **71**, 1695 (1999), C. Binns, Surf. Sci. Rep., **4**, 1 (2001).
  - <sup>3</sup> G. Betz and W. Husinsky, Nucl. Instrum. Methods Phys. Res. **B122**, 311 (1997), M. Moseler, O. Rattunde, J. Nordiek, and H. Haberland, Nucl. Instrum. Methods Phys. Res. **B164-165**, 522 (2000), F. J. Palacios, M. P. Iniguez, M. J. López, and J. A. Alonso Phys. Rev. **B62**, 16031-16039 (2000), L. Bardotti, B. Prüel, P. Minon, A. Perez, Q. Hou, and M. Hou Phys. Rev. **B62**, 2835-2842 (2000), C. Anders, H. M. Urbassek, and R. E. Johnson Phys. Rev. B **70**, 155404 (2004).
  - <sup>4</sup> T. Järvi, A. Kuronen, K. Meinander, K. Nordlund, Phys. Rev. **B75**, 115422 (2007).
  - <sup>5</sup> S. Zimmermann and H. M. Urbassek Phys. Rev. **A74**, 063203 (2006).
  - <sup>6</sup> S. Pratontep, P. Preece, C. Xirouchaki, R. E. Palmer, C. F. Sanz-Navarro, S. D. Kenny, and R. Smith Phys. Rev. Lett. **90**, 055503 (2003).
  - <sup>7</sup> S. J. Carroll, P. D. Nellist, R. E. Palmer, S. Hobday, and R. Smith, Phys. Rev. Lett. **84**, 2654 (2000).
  - <sup>8</sup> V. N. Popok and E. E. B. Campbell, Rev. Adv. Mater. Sci., **11**, 19 (2006).
  - <sup>9</sup> N. Weiss, T. Cren, M. Epple, S. Rusponi, G. Baudot, S. Rohart, A. Tejeda, V. Repain, S. Rousset, P. Ohresser, F. Scheurer, P. Bencok, and H. Brune, Phys. Rev. Lett. **95**, 157204 (2005).
  - <sup>10</sup> H.-G. Boyen, G. Kästle, F. Weigl, B. Koslowski, C. Dietrich, P. Ziemann, J. P. Spatz, S. Riethmüller, C. Hartmann, M. Möller, G. Schmid, M. G. Garnier, P. Oelhafen, Science **297**, 1533 (2002).
  - <sup>11</sup> J. Schmelzer, Jr., S. A. Brown, A. Wurl, M. Hyslop, R. J. Blaikie, Phys. Rev. Lett. **88**, 226802-1 (2002).
  - <sup>12</sup> C. Massobrio, P. Blandin, Phys. Rev. **B47**, 13687 (1993), G. Vandoni, C. Félix, and C. Massobrio Phys. Rev. **B54**, 1553 (1996), G. Vandoni, C. Félix, C. Goyhenex, R. Monot, J. Buttet and W. Harbich, Surface Science, **331-333**, 883 (1995).
  - <sup>13</sup> C. G. Zimmermann, M. Yeadon, K. Nordlund, J. M. Gibson, R. S. Averback, U. Herr, and K. Samwer, Phys. Rev. Lett. **83**, 1163 (1999), J. Frantz, K. Nordlund, Phys. Rev. **B67**, 075415-1 (2003).
  - <sup>14</sup> V. S. Stepanyuk, D. V. Tsivline, D. I. Bazhanov, W. Hergert, and A. A. Katsnelson, Phys. Rev. **B63**, 235406 (2001).
  - <sup>15</sup> S. Padovani, I. Chado, F. Scheurer, and J. P. Bucher, Phys. Rev. **B59**, 11887 (1999).
  - <sup>16</sup> X. Hu, D. G. Cahill, R. S. Averback, J. Appl. Phys. **92**, 3995 (2002).
  - <sup>17</sup> E. Vasco, J. L. Sacedón, Phys. Rev. Lett., **98**, 036104-1 (2007).
  - <sup>18</sup> W.D. Luedtke and U. Landman, Phys. Rev. Lett. **82**, 3835 (1999).
  - <sup>19</sup> P. Süle, J. Chem. Phys. (2008), in press, preprint: [www.mfa.kfki.hu/~sule/papers/ptonal.pdf](http://www.mfa.kfki.hu/~sule/papers/ptonal.pdf).
  - <sup>20</sup> P. Süle, M. Menyhárd, L. Kóti, J. Lábár, W. F. Egelhoff Jr., J. Appl. Phys., **101**, 043502 (2007).
  - <sup>21</sup> F. Baletto, R. Ferrando, Rev. Mod. Phys., **77**, 371 (2005).
  - <sup>22</sup> P. Süle, M. Menyhárd, Phys. Rev., **B71**, 113413 (2005), P.



- Süle, M. Menyhárd, K. Nordlund, Nucl Instr. and Meth. in Phys. Res., **B226**, 517 (2004), **B211**, 524 (2003).
- <sup>23</sup> P. Süle, Surf. Sci., **585**, 170 (2005).
- <sup>24</sup> H. Bulou, J-P. Bucher, Phys. Rev. Lett. **96**, 076102 (2006).
- <sup>25</sup> P. Deltour, J.-L. Barrat, and P. Jensen, Phys. Rev. Lett. **78**, 4597 (1997).
- <sup>26</sup> F. Cleri and V. Rosato, Phys. Rev. **B48**, 22-33 (1993), V. Rosato, M. Guillope, B. Legrand, Phil. Mag. **A59**, 321 (1989).
- <sup>27</sup> K. Nordlund, Comput. Mater. Sci, **3**, 448. (1995),
- <sup>28</sup> H. J. C. Berendsen, J. P. M. Postma, W. F. van Gunsteren, and J. R. Haak, J. Chem. Phys., **81**, 3684 (1984).
- <sup>29</sup> [http://www.mfa.kfki.hu/~sule/\\_/cluster.htm](http://www.mfa.kfki.hu/~sule/_/cluster.htm).
- <sup>30</sup> H. de Waal, R. Pretorius, Nucl. Instr. and Meth. in Phys. Res., **B158**, 717 (1999).
- <sup>31</sup> M. J. Frisch, G. W. Trucks, H. B. Schlegel, *et al.*, Gaussian, Inc., Pittsburgh PA, (2003), see also at: <http://www.gaussian.com>.
- <sup>32</sup> P. Hohenberg and Kohn, Phys. Rev. **136**, 864 (1964), W. Kohn and L. J. Sham, Phys. Rev. **140**, 1133 (1965).
- <sup>33</sup> P. J. Hay, W. R. Wadt, J. Chem. Phys., **82**, 6026 (1985).
- <sup>34</sup> J. P. Perdew, K. Burke, and M. Ernzerhof, Phys. Rev. Lett. **77**, 3865 (1996).
- <sup>35</sup> P. Süle and Á. Nagy, J. Chem. Phys. **104**, 8524 (1996).
- <sup>36</sup> N. Levantov, V. S. Stepanyuk, W. Hergert, O. S. Trushin, K. Kokko, Surf. Sci., **400**, 54 (1998).
- <sup>37</sup> P. Süle, M. Menyhárd, K. Nordlund, Nucl Instr. and Meth. in Phys. Res., **B222**, 525 (2004).
- <sup>38</sup> D. L. Beke, Z. Erdélyi, Phys. Rev. **B73**, 035426 (2006).